



# Spatial distribution of soil organic carbon in the ecologically fragile Horqin Grassland of northeastern China

Yuqiang Li<sup>a,\*</sup>, Xuyang Wang<sup>a,b</sup>, Yayi Niu<sup>a,b</sup>, Jie Lian<sup>a</sup>, Yongqing Luo<sup>a</sup>, Yinping Chen<sup>c</sup>,  
Xiangwen Gong<sup>a,b</sup>, Huan Yang<sup>a</sup>, Peidong Yu<sup>c</sup>

<sup>a</sup> Northwest Institute of Eco-Environment and Resources, Chinese Academy of Sciences, Lanzhou 730000, China

<sup>b</sup> University of Chinese Academy of Sciences, Beijing 100049, China

<sup>c</sup> School of Environmental and Municipal Engineering, Lanzhou Jiaotong University, Lanzhou 730070, China

## ARTICLE INFO

Handling Editor: Dr David Laird

### Keywords:

Sandy grassland  
Desertification  
Carbon stock  
Spatial pattern  
Horqin Sandy Land

## ABSTRACT

The spatial distribution of soil organic carbon (SOC) and its storage in the topmost 100 cm of the soil were investigated in the Horqin Grassland of northeastern China. Soil samples were collected at 1465 sites, covering  $12.03 \times 10^4 \text{ km}^2$ . The region had a mean SOC density of  $6.84 \text{ kg C m}^{-3}$ , which is lower than China's mean ( $9.60 \text{ kg C m}^{-3}$ ) and the world's mean ( $10.40 \text{ kg C m}^{-3}$ ). The mean SOC density was much higher in the northern part of the study area ( $8.85 \text{ kg C m}^{-3}$ ) than in the southern part ( $4.84 \text{ kg C m}^{-3}$ ). The total SOC storage in the Horqin Grassland was  $862.74 \text{ Tg}$ . SOC storage decreased with increasing soil sampling depth. The SOC stored in the top 10, 20, 40, and 60 cm accounted for 17.7, 31.7, 53.8, and 71.3%, respectively, of the total amount in the top 100 cm. The region's extensive desertification appears to be one of the most important factors that led to the relatively low SOC content and the difference between the northern and southern parts of the Horqin Grassland. Our results provide an important baseline for evaluating past losses of SOC due to desertification, and for projecting the potential increase in SOC from the restoration of desertified land and how SOC will respond to climate change.

## 1. Introduction

A large quantity of organic carbon is stored in the soil of the world's terrestrial ecosystems. The soil organic carbon (SOC) pool in the top 100 cm totals about 1550 Pg, which is about twice the size of the atmospheric pool and three times the size of the biotic pool (Lal, 2004a). Against the background of global warming, the relatively large size and long residence time of the SOC pool make it an important sink for carbon released into the atmosphere by anthropogenic activities (Post et al., 1982). Changes in SOC storage are now taken into account in international negotiations regarding climate change (Martín et al., 2011). SOC and its potential to mitigate the build-up of atmospheric carbon dioxide ( $\text{CO}_2$ ) through soil carbon sequestration have attracted considerable scientific attention (Jobbágy and Jackson, 2000; Lal, 2004b; Smith et al., 2008; Schrumpf et al., 2011; Grüneberg et al., 2014; O'Rourke et al., 2015; Deng and Shangquan, 2017).

Accurate estimates of SOC storage and its changes are necessary to support improved carbon management and climate change mitigation, as well as to help parameterize the carbon cycle models that are being used to guide climate policy (Schrumpf et al., 2011; Scharlemann et al.,

2014). Many studies have estimated SOC storage at regional (Yang et al., 2009; Wiesmeier et al., 2015), national (Kern, 1994; Yu et al., 2007; Martín et al., 2011), and global (Post et al., 1982; Mitra et al., 2005; Scharlemann et al., 2014) scales. However, high uncertainty is associated with the estimates, especially for global SOC storage, because of inconsistent methods and limited data for many regions. Most studies have estimated global SOC at roughly 1500 Pg in the topmost 100 cm of the soil, but estimates range from 504 to 3000 Pg (Scharlemann et al., 2014). The estimates of SOC storage for the contiguous United States range from 62.1 to 99.3 Pg (Kern, 1994), whereas estimates for China's terrestrial ecosystems range from 50 to 180 Pg (Yu et al., 2007) and estimates for global wetlands range from 202 to 535 Pg (Mitra et al., 2005).

The inconsistencies among studies highlight the need for more detailed regional-level measurements of SOC storage and its spatial distribution through *in situ* sampling. SOC levels depend on local climatic conditions and other site-specific conditions, as well as on the type of land-use and land management (Yu et al., 2007). Thus, spatially explicit databases obtained from *in situ* measurements are important to help researchers establish the relationships between the geographical

\* Corresponding author at: Northwest Institute of Eco-Environment and Resources, Chinese Academy of Sciences, 320 Donggang West Road, Lanzhou 730000, China.  
E-mail address: [liyq@lzb.ac.cn](mailto:liyq@lzb.ac.cn) (Y. Li).

distribution of SOC and the climate, vegetation, human development, and other factors that affect this distribution; such data provides the basis for assessing the influence of changes in any of these factors on the carbon cycle (Post et al., 1982). However, despite a great deal of research on SOC, there currently remains substantial uncertainty on the size of the SOC storage, its spatial distribution, and carbon emissions from soils (Scharlemann et al., 2014).

The Horqin Grassland is one of the largest grasslands in China. However, this region has undergone serious aeolian desertification in recent decades. The area of desertified land accounted for 77.6% of the total area in the late 1980s (Liu et al., 1996). There is a strong link between desertification and the emission of CO<sub>2</sub> from the soil and vegetation (Lal, 2001). Arid and semi-arid regions have been regarded as having high potential as carbon sinks due to the large global extent and widespread desertification of these regions (Nosetto et al., 2006). Therefore, more and more researchers have studied carbon sequestration in severely desertified areas through strategies such as afforestation (Cao et al., 2008; Li et al., 2013, 2017) and grazing exclusion (Li et al., 2012), as well as carbon and nitrogen losses due to desertification (Zhou et al., 2008) and carbon and nitrogen storage in various land uses (Li et al., 2014) in the Horqin Grassland. However, these studies were only conducted in limited areas and none investigated, in detail, the spatial distribution of SOC and its storage throughout this area.

In this paper, we present the results of the largest field study to date in the Horqin Grassland to obtain details of the spatial distribution of SOC and estimate its storage. We tested the following hypotheses: (1) that the Horqin Grassland would have a relatively low SOC density, primarily due to widespread desertification in the region; and (2) that the SOC distribution would be affected by climatic and topographic factors. The results from this study can provide a baseline for evaluating future changes in SOC storage in the Horqin Grassland and data for the parameterization of regional models that can be used to predict the SOC dynamics induced by climate change and changes in the land-use and cover type.

## 2. Materials and methods

### 2.1. Study area

The Horqin Grassland (also called the Horqin Sandy Grassland or the Horqin Sandy Land) is located in the western part of northeastern China. The present study area, which covers 13 counties of China's Inner Mongolia autonomous region, has an area of  $12.03 \times 10^4$  km<sup>2</sup>. It ranges between 41°40'38"N and 46°3'25"N and between 117°52'12"E and 123°42'48"E (Fig. 1). The Xiliao River crosses this region from west to east and separates it into two parts: the northern part is characterized by alluvial flood plains and sloping piedmont plains, whereas the southern part is characterized by sand dunes that alternate with gently undulating interdunal lowlands (Li et al., 2017). The study area is a typical temperate grassland of the Central Asian Steppe ecosystem, with a continental semiarid monsoon temperate climate. Elevation ranges from 90 to 1625 m above sea level. Mean annual air temperature is 3 to 7 °C. Mean monthly temperatures vary from a minimum of −12.6 to −16.8 °C in January to a maximum of 20.3 to 23.5 °C in July. The annual frost-free period is approximately 140 to 160 days. The mean annual precipitation is 350 to 500 mm, with the highest values in the summer from June to August (Duan et al., 2014).

The zonal soils are classified as Kastanozems, Chernozems, and Luvisols based on the Food and Agriculture Organization of the United Nations soil classification system (FAO, 2006), but the current dominant soils are Arenosols as a result of desertification. The native vegetation mainly consists of mesoxerophytes characterized by palatable grass species along with sparsely scattered woody species (Li et al., 2017). However, the vegetation has been degraded seriously during the past century by extensive desertification, which has been caused by a combination of climate change and unsustainable land use. As a result,

the area has become dominated by xerophytes and psammophytes (Liu et al., 1996).

### 2.2. Soil sampling and measurement methods

Soil samples were manually collected from five layers (0 to 10, 10 to 20, 20 to 40, 40 to 60, and 60 to 100 cm) using a 2.5-cm-diameter soil auger. Because of the huge study area, sampling was very expensive and very labor- and time-consuming. Therefore, soil samples were collected over a 7-year period from 2011 to 2017. Soil sampling in Naiman County was conducted from July to August 2011, whereas the other 12 counties were sampled from April to August from 2014 to 2017.

We originally intended to collect soil samples from each 10 km × 10 km cell in the study area. However, soil samples were collected at intervals of < 10 km for some sites with high spatial heterogeneity and at intervals of > 10 km for some sites with large areas of mountains and sand dunes. In the end, we selected a total of 1465 locations (733 in the northern part and 732 in the southern part) for soil sampling within the study area. The mean sampling interval was 6.65 km. One 10 m × 10 m plot was established at each of the 1465 locations. The soil samples were collected randomly at 15 sampling points within each plot and bulked to prepare a composite sample for each layer. Therefore, we obtained five composite samples (one per depth range) to a depth of 100 cm within each plot, yielding a total of 7325 composite samples.

Three additional sampling points (replicates) in each plot were selected to determine the soil bulk density, using a soil auger equipped with a stainless steel cylinder (100 cm<sup>3</sup> in volume) to sample intact soil cores at 10-cm intervals. This work is more arduous than the work to collect composite soil samples. Because of high variation in the soil texture and water conditions, it was difficult to collect intact soil cores to a depth of 100 cm using this method. Therefore, a single soil bulk density value was calculated for a combined layer down to 100 cm depth at a given location, which represents the average of 5 to 10 soil cores at each point.

In the laboratory, soil samples for determination of the SOC concentration were air-dried, hand-sieved (through a 2-mm mesh), hand-picked to remove fine roots and other debris, and then ground to pass through a 0.25-mm mesh. Where it was not possible to insert the soil sampler into the soil, or where the sampler encountered an obstacle (e.g., a stone) larger than the sampler's diameter (2.5 cm), it would have been prohibitively difficult to collect a full sample at that location, so we repositioned the sampler to a nearby location. Where coarse fragments smaller than the sampler diameter were included in the sample, we accounted for their volumetric percentage of the sample in our calculations. This affected a total of only 4.1% of our samples. We used the Walkley-Black dichromate oxidation procedure (Nelson and Sommers, 1982) to determine the SOC concentration.

### 2.3. Data acquisition for factors that influenced SOC

The land-use type, geographical coordinates, and elevation were recorded for each of the 1465 sample locations using a GPS receiver. We created a dataset that included the slope, slope aspect, aridity index (evaporation/precipitation), Thornthwaite's moisture index, mean annual precipitation, and mean annual air temperature, averaged from 1980 to 2015, and values of the normalized-difference vegetation index (NDVI) in 2015 for each sampling location, as well as the areas of the different land-use types in 2015 for each county. Data were obtained from the Resources and Environmental Sciences Data Center, Chinese Academy of Sciences (RESDC, 2017).

### 2.4. Estimation of SOC density and storage

For each county, SOC density (SOC<sub>D</sub>, in kg C m<sup>−3</sup>) was estimated using Eq. (1) and SOC storage (SOC<sub>S</sub>, in Tg) was estimated using Eq.

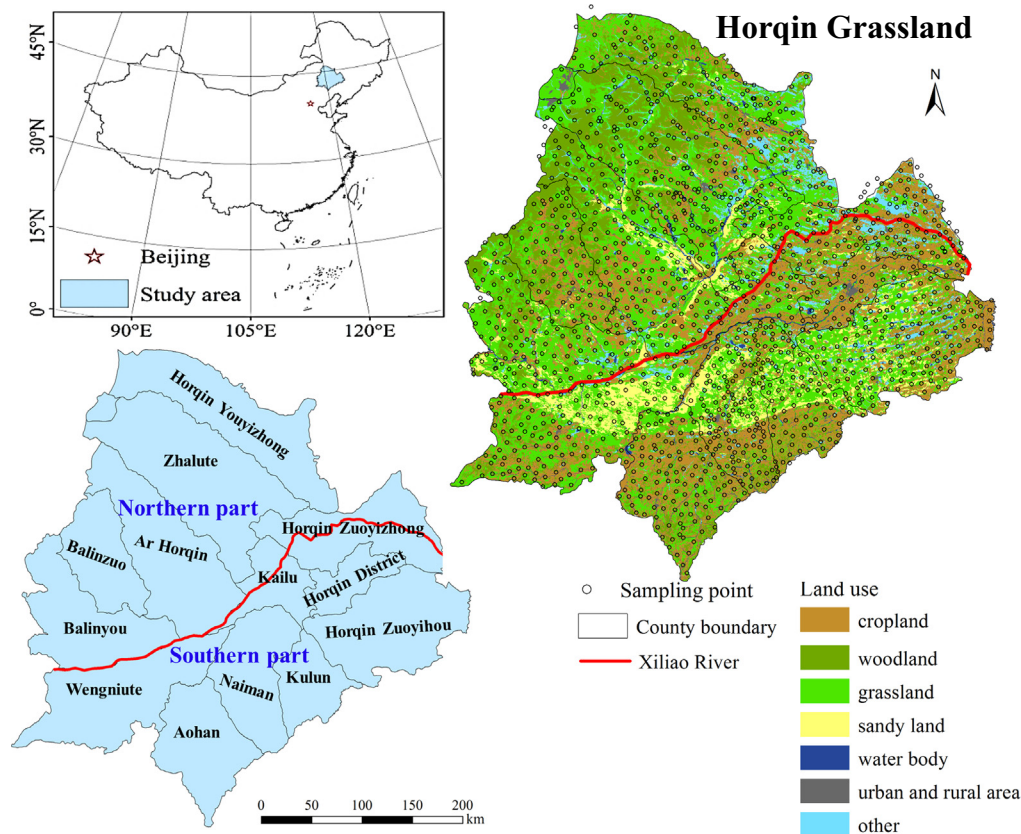


Fig. 1. Locations of the Horqin Grassland and of the soil sampling points ( $n = 1465$ ). The region is divided into northern and southern parts by the Xiliao River.

(2), both to a depth of 100 cm:

$$SOCD = SOCC \times BD \times (1 - [cf/100]) \quad (1)$$

$$SOCS = 0.001 \times A \times SOCD \quad (2)$$

where  $SOCC$  represents the SOC concentration (in  $\text{g kg}^{-1}$ ),  $BD$  represents the soil bulk density (in  $\text{g cm}^{-3}$ ),  $cf$  represents the volumetric percentage of coarse fragments ( $> 2 \text{ mm}$ ) in the soil (Cools and De Vos, 2010), 0.001 represents a unit conversion factor, and  $A$  represents the area of a given county (in  $\text{km}^2$ ). SOC storage for the whole study area equaled the sum of the storage in each of the 13 counties.

## 2.5. Statistical and geostatistical methods

The descriptive statistical parameters, correlations between parameters, normality tests, homogeneity of variance tests, and regression analyses were performed using version 20.0 of the SPSS software. Testing for a normal distribution and homogeneity of variance were performed using the Kolmogorov–Smirnov test and Levene's test, respectively, at a significance level of 0.05. For individual soil layers and for the combined layer from 0 to 100 cm in both the northern and the southern parts of the study area, the SOC concentrations did not pass the normality test and the probability distributions were positively skewed and had a sharp peak (positive kurtosis values). However, ln-transformation of the raw data created a better fit to a normal distribution (Table S1). We used the ln-transformed datasets for SOC concentrations and the raw datasets for  $BD$  in the following multivariate analyses. Table S2 summarizes the statistical characteristics of the SOC and  $BD$  data. Fig. S1 shows histograms with a normal distribution and probability–probability (P-P) plots of the mean SOC concentrations to a depth of 100 cm.

Pearson's correlation coefficient ( $r$ ) was applied to confirm the strength of the correlations between parameters. One-way ANOVA

combined with least-significant-difference (LSD) tests were used to identify significant differences in the measured soil variables among soil layers as well as between the northern and southern parts of the study area. The geostatistical analyses were performed and the spatial distribution maps of SOC density were produced using version 10.3 of the ArcGIS software. We used ordinary kriging with the parameters of an exponential model to interpolate between data points.

## 3. Results

### 3.1. Spatial distribution of SOC

The SOC concentrations for the combined layer from 0 to 100 cm ranged from  $0.30$  to  $45.54 \text{ g kg}^{-1}$ , with an arithmetic mean of  $8.64 \text{ g kg}^{-1}$ , in the northern part of the study area, versus from  $0.19$  to  $19.87 \text{ g kg}^{-1}$ , with an arithmetic mean of  $4.13 \text{ g kg}^{-1}$ , in the southern part. The mean SOC concentration for the combined layer from 0 to 100 cm in the northern part was therefore 2.1 times the value in the southern part. The patterns of vertical variation showed that SOC concentrations decreased with increasing depth in both parts of the study area (Fig. 2). Except for the lack of a significant difference between the 40 to 60 cm layer and the 60 to 100 cm layer in the southern part of the study area, the SOC concentrations differed significantly between any two soil layers within a given part of the study area. Comparison of the two parts indicated that the SOC concentration was significantly higher at all depths in the northern part of the study area.

The highest SOC densities were located in the areas with mountain woodland and grassland in the northern part of the study area, whereas the lowest were located in the areas with active sand dunes in the southern part (Fig. 3). The average SOC density to a depth of 100 cm for the northern part ( $8.85 \text{ kg C m}^{-3}$ ) was 82.9% higher than the value for the southern part ( $4.84 \text{ kg C m}^{-3}$ ). For the overall study area, SOC density decreased significantly with increasing depth in the soil, with

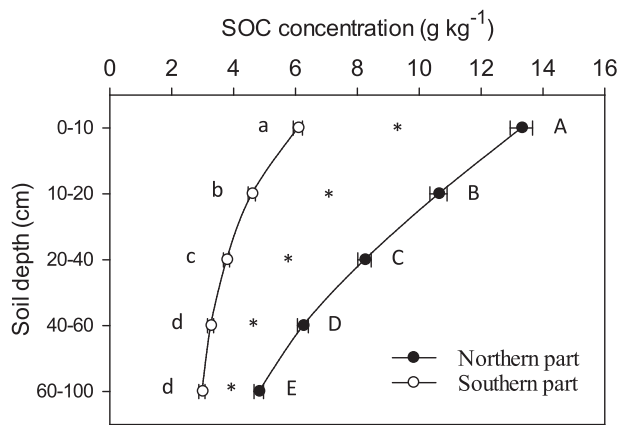


**Fig. 2.** Changes in the soil organic carbon (SOC) concentration with increasing depth in soils of the northern part ( $n = 733$ ) and southern part ( $n = 732$ ) of China's Horqin Grassland. Values represent means  $\pm$  standard errors (SE). Points labeled with different uppercase letters differed significantly ( $P < 0.05$ ) between soil layers in the northern part; points labeled with different lowercase letters differed significantly ( $P < 0.05$ ) between soil layers in the southern part; and the \* between two lines indicates a significant difference between the northern and southern parts for a given soil layer.

values ranging from  $12.09 \text{ kg C m}^{-3}$  in the 0 to 10 cm layer to  $4.95 \text{ kg C m}^{-3}$  in the 60 to 100 cm layer, with an average of  $6.84 \text{ kg C m}^{-3}$  for the topmost 100 cm of the soil.

For both the northern and southern parts of the study area, changes in SOC density to a depth of 100 cm as a function of latitude showed similar trends that could be described by a statistically significant concave-up quadratic equation (Fig. 4). Changes in SOC density as a function of longitude could also be significantly fitted by a quadratic equation in both parts of the study area, but the parabola opened downward in the northern part and upward in the southern part (Fig. 4).

The average SOC densities to a depth of 100 cm for each county (Table 1) showed that Balinzuo County, in the northern part, had the highest value, at  $10.91 \text{ kg C m}^{-3}$ ; the dominant land-use type in this county was woodland. In contrast, Kulun County, in the southern part, had the lowest value, at  $3.35 \text{ kg C m}^{-3}$ ; this county was the most-severely desertified part of the study area. The SOC storage to a depth of 100 cm for each county ranged from 15.54 Tg in Kulun County to 179.55 Tg in Zhazlut County, with a total of 862.74 Tg for the study area. The proportion of the total SOC storage accounted for by the layer from 0 to 10 cm was 17.7%, versus 31.7% for the combined layers from 0 to 20 cm, 53.8% for the combined layers from 0 to 40 cm, and 71.3% for the combined layers from 0 to 60 cm.

### 3.2. Relationships between SOC density and other factors

We calculated the values of Pearson's correlation coefficient for the relationships between SOC density to a depth of 100 cm and nine environmental factors (Table 2). In both parts of the study area, SOC density was significantly positively correlated with elevation, slope, and NDVI, but significantly negatively correlated with the aridity index, mean annual air temperature, and soil bulk density; we found no significant correlation between SOC density and slope aspect. SOC density had a highly significant positive correlation with Thornthwaite's moisture index and mean annual precipitation in the northern part of the study area, but not in the southern part. To facilitate the use of this data by modelers, we also performed regression analysis for the relationships between SOC density and each of the nine environmental factors in both the northern and southern parts of the study area (Fig. S2).

Fig. 5 shows the relationship between the average SOC density in

each county as a function of the proportion of woodland (forest, shrubland, and sparse woodland) and the proportion of sandy land (land dominated by active sand dunes with vegetation cover  $< 5\%$ ). SOC density increased significantly ( $P < 0.01$ ) with an increasing proportion of woodland, but decreased significantly ( $P < 0.05$ ) with an increasing proportion of sandy land. We found no significant relationship between the SOC density and the proportion of cropland or grassland.

## 4. Discussion

### 4.1. SOC density and its vertical distribution

Our results suggest that the Horqin Grassland had a relatively low mean SOC density to a depth of 100 cm ( $6.84 \text{ kg C m}^{-3}$ ). The world's mean SOC density to a depth of 100 cm is about  $10.40 \text{ kg C m}^{-3}$  (Foley, 1995). The most detailed and reliable research on regional patterns of SOC density in China until the present study was based on data from 7292 soil profiles collected across the country in the mid-1980s (Yu et al., 2007); the authors reported a mean SOC density of  $9.60 \text{ kg C m}^{-3}$  to a depth of 100 cm and placed the estimates in the following regional order: Northeast China ( $18.19$ )  $>$  Southwest China ( $10.38$ )  $>$  Taiwan–Hong Kong–Macau region ( $10.28$ )  $>$  Central-south China ( $9.82$ )  $>$  North China ( $9.12$ )  $>$  East China ( $8.30$ ).

Most regional studies reported a greater SOC density to a depth of 100 cm than in our study. For example, SOC density in the upper Rio Negro basin of the Amazon region reached  $86.80 \text{ kg C m}^{-3}$  (Montes et al., 2011). A region of the Zoige alpine wetland in China's northeastern Qinghai–Tibet Plateau had a mean SOC density of  $63.80 \text{ kg C m}^{-3}$  (Ma et al., 2016). The mean SOC density was  $34.80 \text{ kg C m}^{-3}$  in North America's Arctic region (Chien et al., 2008). The northern circumpolar permafrost region had a mean SOC density of  $26.40 \text{ kg C m}^{-3}$  (Tarnocai et al., 2009). The SOC density for the main land use types in southeastern Germany ranged from  $9.00$  to  $11.80 \text{ kg C m}^{-3}$  (Wiesmeier et al., 2012). The mean SOC density was  $7.70 \text{ kg C m}^{-3}$  across China's Loess Plateau region (Liu et al., 2011). However, a few studies reported a lower SOC density than ours. China's alpine grasslands and desertified land had a mean SOC density of  $6.50 \text{ kg C m}^{-3}$  (Yang et al., 2008) and  $2.32 \text{ kg C m}^{-3}$  (Feng et al., 2002), respectively.

A distinct feature of the vertical distribution in the present study was that SOC content decreased with increasing depth in the soil (Fig. 2). This was consistent with the results from many previous studies (Wang et al., 2004; Lorenz and Lal, 2005; Cunningham et al., 2012; Ma et al., 2016). The primary and secondary sources of SOC formation are plant litter and microbial residues, respectively (Lorenz and Lal, 2005). Therefore, climate, plant functional types, and the relative allocations of photosynthate to shoots and roots, together with the vertical root distribution, are the most important factors that define the vertical distribution of SOC (Jobbágy and Jackson, 2000; Wang et al., 2004). Globally, the percentages of SOC in the top 20 cm of the soil (relative to the top 100 cm) were 42.0% for grassland, 50.0% for forest, and 33.0% for shrubland (Jobbágy and Jackson, 2000). For China's terrestrial ecosystems, the SOC stored in the top 10, 20, 30, 50, and 100 cm of the soil accounted for 22.0, 41.0, 54.0, 74.0, and 100.0% of the total, respectively (Wang et al., 2004). In the present study, the SOC stored in the top 10, 20, 40, and 60 cm accounted for 17.7, 31.7, 53.8, and 71.3%, respectively, of the total amount in the top 100 cm.

### 4.2. Relationships between SOC and environmental and anthropogenic factors

The natural spatial distribution of SOC and the potential capacity for SOC storage are predominantly controlled by climate, biome, topography, and soil parent material, but climate is the most important factor (Jobbágy and Jackson, 2000; Luo et al., 2017). Previous regional

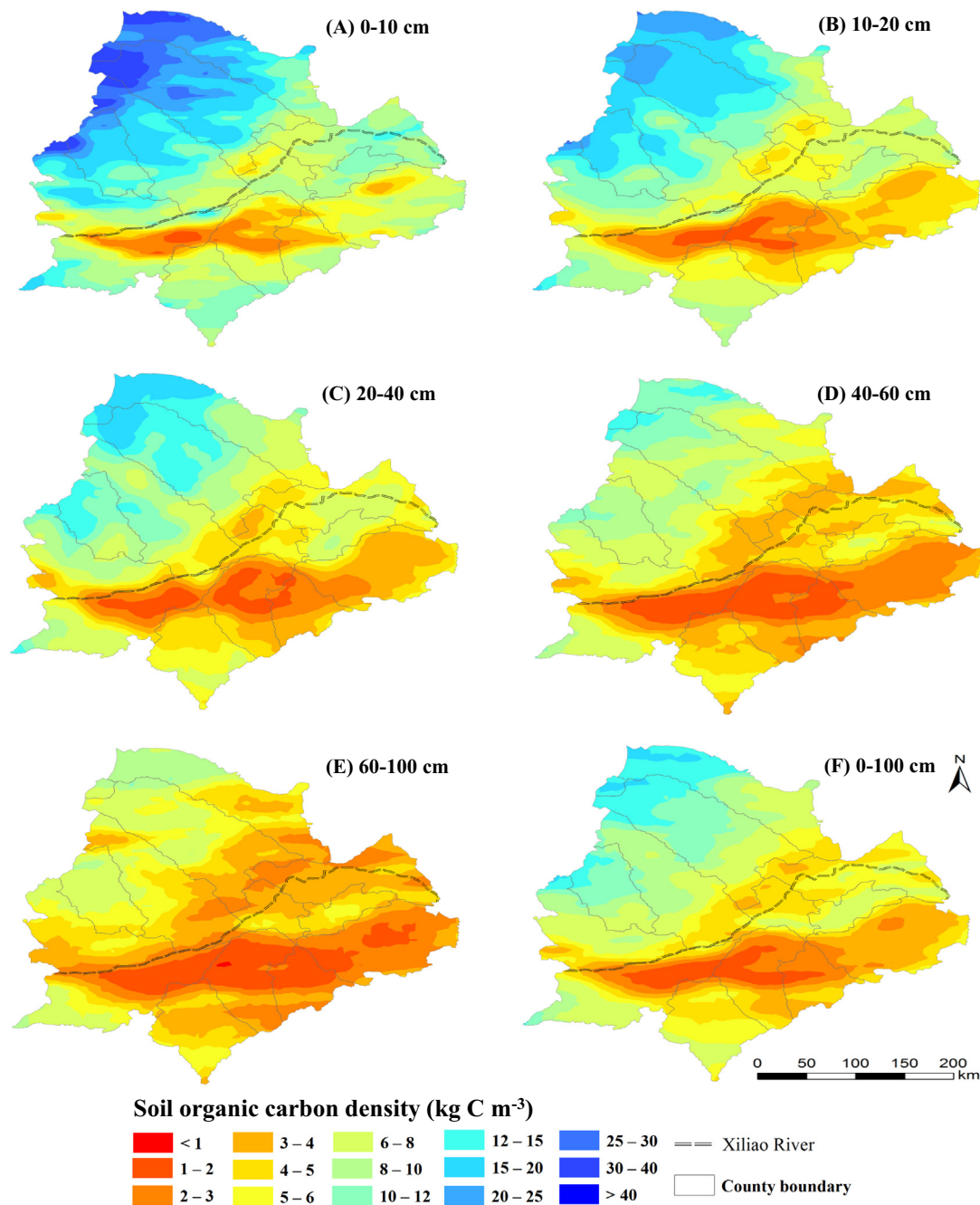
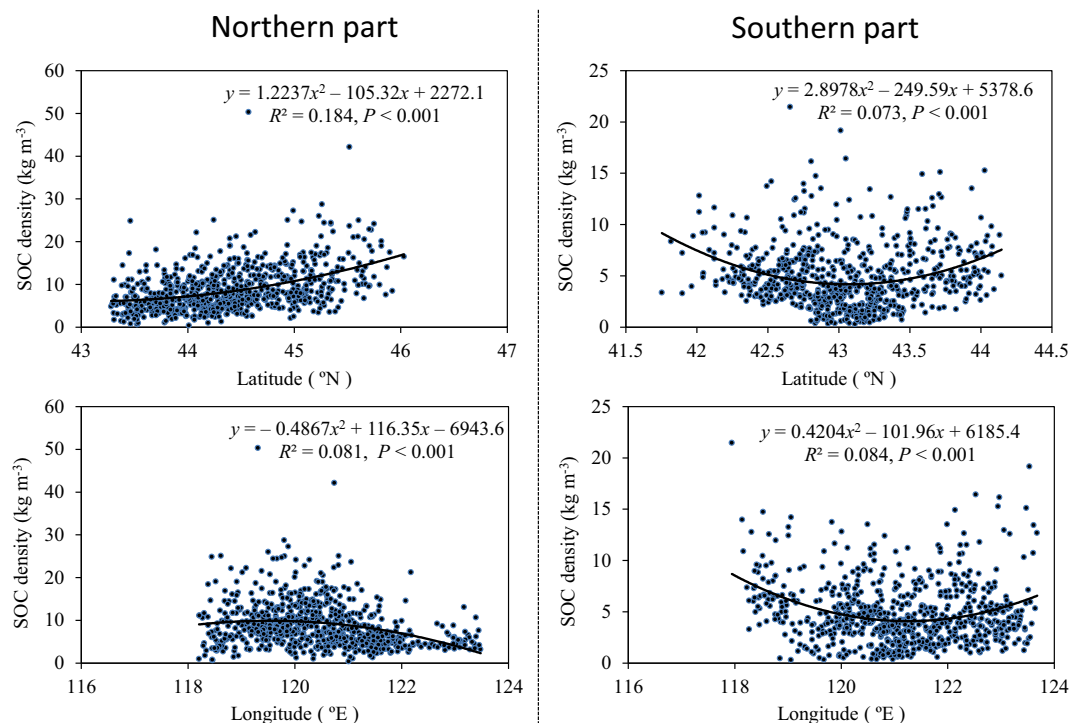


Fig. 3. Spatial distribution of the soil organic carbon (SOC) density for individual soil layers and for the combined layer from 0 to 100 cm.

studies (McGrath and Zhang, 2003; Gao et al., 2013) have clarified that SOC was significantly positively correlated with elevation, because high elevation tends to result in increased precipitation and decreased temperature, and thus tends to favor the accumulation of SOC. The studies by Liu et al. (2006) and Zhang et al. (2012) also reported that slope aspect can significantly affect the SOC level; northern-hemisphere sites on north-facing slopes receive less solar radiation, leading to cooler temperatures and slower decomposition of SOC. In addition, steeper slopes tend to result in more water erosion, leading to increased removal of organic matter and decreased SOC (Liu et al., 2006). In the present study, SOC density was significantly positively correlated with elevation, slope, and NDVI, but was significantly negatively correlated with aridity index, mean annual air temperature, and bulk density in both the northern and southern parts of the study area (Table 2). However, SOC density was significantly positively correlated with

mean annual precipitation and Thornthwaite's moisture index in the northern part, but not in the southern part.

Anthropogenic activity (positive or negative) has become a critical factor for the evolution of SOC (Lal, 2004a). Desertification decreases the total soil carbon storage and transfers carbon from the soil to the atmosphere (Lal, 2001); because this severe type of land degradation is driven by both natural and human factors, solutions must include responses to both processes such as climate change and to human factors such as unsustainable land uses. The extensive desertification that has occurred in the Horqin Grassland is likely to be one of the most important factors that is responsible for the relatively low SOC level in this region, as well as for the differences in SOC density between the northern and southern parts (Fig. 3). This would also explain the differences in the relationships between SOC and precipitation and Thornthwaite's moisture index (Table 2) and differences in the SOC



**Fig. 4.** Relationships between soil organic carbon (SOC) density to a depth of 100 cm and the latitude and longitude of the sampling sites in the northern part ( $n = 733$ ) and southern part ( $n = 732$ ) of China's Horqin Grassland.

**Table 1**

Densities and storage of soil organic carbon (SOC) to a depth of 100 cm for each county and for the whole study area.

County	Area (km <sup>2</sup> )	SOC density (kg C m <sup>-3</sup> )	SOC storage (Tg C)
Balinzuo	6463.58	10.91	70.54
Zhalute	17,197.76	10.44	179.55
Horqin Youyizhong	12,289.21	10.24	125.88
Ar Horqin	12,768.33	8.26	105.53
Balinyou	9826.48	7.71	75.74
Horqin District	3498.77	7.40	25.88
Wengniute	11,864.96	5.58	66.15
Horqin Zuoyizhong	9502.40	5.56	52.82
Aohan	8263.48	5.50	45.45
Kailu	4223.24	5.21	22.01
Horqin Zuoyihou	11,541.90	4.17	48.15
Naiman	8174.73	3.61	29.50
Kulun	4638.93	3.35	15.54
Total study area	120,253.80	6.84 <sup>a</sup>	862.74

<sup>a</sup> A weighted average based on the SOC density of each county and its area.

trends with respect to latitude and longitude (Fig. 4). Our previous research in the study area (Li et al., 2006) found that along the spectrum from non-desertification to extremely severe desertification, SOC storage in grassland to a depth of 100 cm decreased by 90.0%. Zhou et al. (2008) estimated that desertification in the Horqin Grassland resulted in a loss of 101.62 Tg of SOC to a depth of 100 cm during the last century. This amount accounted for 11.8% of the current total SOC storage (862.74 Tg) estimated in the present study.

Yu et al. (2007) suggested that farmland had a higher SOC density than grassland in their study because they included desertified grassland in northwest China in the grassland ecosystem. But if we compare the map of the spatial distribution of desertified land in the study area in 2010 (Duan et al., 2014) with the present map of the spatial distribution of SOC (Fig. 3), we can see that the areas with desertified land overlapped the areas with low SOC density. We have calculated the SOC density for each of four severity categories in Duan's map; the mean

SOC density (kg C m<sup>-3</sup>) decreased with increasing desertification intensity: slight (5.40) > moderate (5.27) > severe (4.90) > extremely severe (3.47). The restoration of extremely severely desertified land in the Horqin Grassland by means of grazing exclusion (Li et al., 2012) and afforestation (Li et al., 2013) has significantly improved SOC storage. If we combine the results of these previous studies with the present results for SOC density in each county, which showed a significant negative relationship between SOC and the proportion of sandy land (Fig. 5B), this supports the hypothesis that increasing severity of desertification is closely linked to decreasing SOC.

In addition, it has been well recognized that replacing natural ecosystems with cultivated fields generally decreases SOC (Guo and Gifford, 2002). McGrath and Zhang (2003) found that the SOC content was significantly negatively correlated with the proportion of cultivated agricultural land for each county in Ireland. We found no significant relationship between the SOC content and the proportion of cropland in the present study. However, cultivation was one of the most important factors associated with desertification of the Horqin Grassland in a previous study (Zhou et al., 2008). If we compare the map of land use (Fig. 1) with the map of the spatial distribution of SOC (Fig. 3), it is nonetheless clear that the larger the area of sandy land and cropland, the lower the SOC density, especially in the southern part of the study area.

In many studies that estimated SOC storage (Post and Kwon, 2000; Xie et al., 2007; Yang et al., 2009), the soil bulk density was generally obtained by using pedotransfer functions. Interestingly, there has been considerable interest in developing more time- and cost-efficient methodologies for SOC prediction using remote sensing data to support the development of pedotransfer functions (Gomez et al., 2008; Yang et al., 2009; Vågen et al., 2016). For example, Yang et al. (2009) used the pedotransfer function between SOC density and NDVI to estimate SOC density in the Tibetan grasslands from satellite observations for each pixel, and used this approach to document changes in the spatial distribution of SOC density between two periods (1980s and 2001–2004). Therefore, our present results provide the basis for future development of potential pedotransfer functions between SOC and bulk

**Table 2**

Correlation coefficients (Pearson's  $r$ ) for the relationships between the soil organic carbon density (SOCD) to a depth of 100 cm and elevation (EL), slope (SL), slope aspect (SA), aridity index (AR, evaporation/precipitation), Thornthwaite's moisture index (IM), mean annual precipitation (PA), mean annual air temperature (TA), normalized-difference vegetation index (NDVI), and soil bulk density (BD) in the northern part (lower-left side of the table) and southern part (upper-right side of the table) of China's Horqin Grassland.

	S OCD	EL	SL	SA	AR	IM	PA	TA	NDVI	BD
S OCD		0.223**	0.195**	0.024	−0.090*	0.043	−0.001	−0.274**	0.396**	−0.497**
EL	0.428**		0.713**	0.083*	0.001	−0.181**	−0.318**	−0.619**	−0.157**	−0.324**
SL	0.367**	0.673**		0.175**	−0.170**	0.057	−0.024	−0.412**	−0.062	−0.370**
SA	0.018	0.140**	0.063		−0.036	0.027	0.033	0.008	0.086*	−0.082*
AR	−0.419**	−0.544**	−0.415**	−0.133**		−0.944**	−0.875**	−0.046	−0.112**	0.150**
IM	0.422**	0.475**	0.337**	0.155**	−0.871**		0.978**	0.195**	0.171**	−0.083*
PA	0.143**	−0.278**	−0.094*	0.085*	−0.483**	0.647**		0.302**	0.207**	−0.048
TA	−0.460**	−0.902**	−0.632**	−0.120**	0.656**	−0.644**	0.071		−0.020	0.212**
NDVI	0.308**	0.176**	0.133**	0.015	−0.287**	0.338**	0.225**	−0.278**		−0.329**
BD	−0.510**	−0.230**	−0.290**	0.056	0.308**	−0.319**	−0.213**	0.292**	−0.259**	

Significance (two-tailed): \*\*,  $P < 0.01$ ; \*,  $P < 0.05$ .

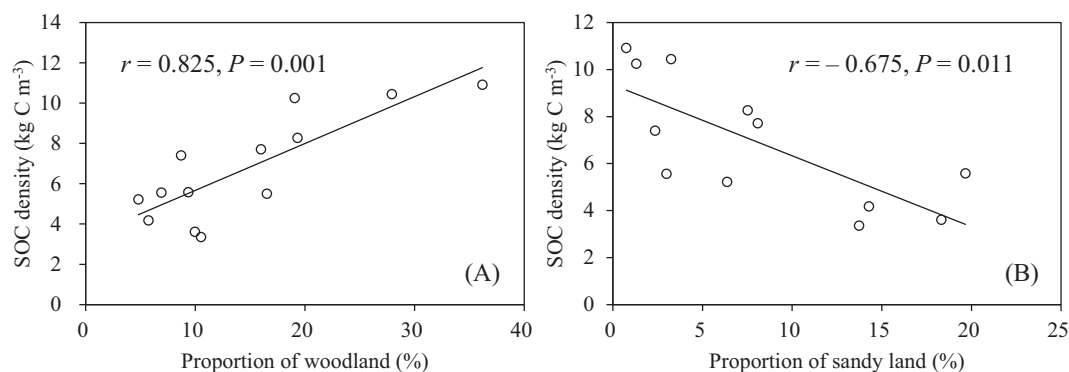


Fig. 5. Average SOC density for each county as a function of the proportions of (A) woodland and (B) sandy land ( $n = 13$ ).

density as well as between SOC and NDVI.

In the present study, we investigated the spatial distribution of SOC to permit a more accurate estimate of the storage by means of the most extensive and highest density of *in situ* soil sampling that has been conducted to date in the Horqin Grassland. The total area of aeolian desertified land has been decreasing and the environmental conditions have been improving in the Horqin Grassland since the early 2000s, due to the impacts of government programs to reverse desertification by planting trees and shrubs and by reducing grazing pressure (Duan et al., 2014). Previous studies (Cao et al., 2008; Li et al., 2012, 2013, 2017) have evaluated the carbon sequestration potential of a range of restoration practices in the region. These studies found that reducing the pressure on the grasslands caused by livestock grazing has stabilized the sands and allowed recovery of the native vegetation. However, these studies were conducted at fewer sites than in the present study. It will be necessary to perform a more comprehensive study to evaluate the loss of SOC due to the desertification that occurred in the past, and to project the gain of SOC that will result from the government's ecological restoration and desertification control programs. In the current context of global climate change, it will also be important to predict how SOC will respond to climate change in the future. For such analyses, our results will provide an important baseline.

## 5. Conclusions

China's degraded Horqin Grassland showed a lower level of SOC than in most other studies around the world. The northern part of our study area had a much higher SOC density than the southern part. Climatic and topographic factors such as the elevation, slope, NDVI, aridity index, temperature, precipitation, and Thornthwaite's moisture index significantly affected the SOC level. SOC showed distinct vertical changes, with SOC decreasing significantly with increasing depth in the

soil. The extensive desertification in the study area is one of the most important factors that have defined the spatial distribution of SOC in the region. The present results provide a valuable baseline for use in evaluating the SOC loss due to past desertification, for estimating the potential increase in SOC sequestration due to restoration of desertified land, and for predicting how SOC will respond to climate change in the future.

Supplementary data to this article can be found online at <https://doi.org/10.1016/j.geoderma.2018.03.032>.

## Acknowledgments

This research was supported by the National Key R & D Program of China (2017YFA0604803), the One Hundred Person Project of the Chinese Academy of Sciences (Y551821), and the National Natural Science Foundation of China (grants 31640012, 31560161, 31260089, and 31400392). We are very grateful to the journal's anonymous reviewers and editors for their constructive comments regarding the manuscript.

## References

- Cao, C.Y., Jiang, D.M., Teng, X.H., Jiang, Y., Liang, W.J., Cui, Z.B., 2008. Soil chemical and microbiological properties along a chronosequence of *Caragana microphylla* Lam. plantations in the Horqin sandy land of northeast China. *Appl. Soil Ecol.* 40, 78–85.
- Chien, L.P., Michaelson, G.J., Jorgenson, M.T., Kimble, J.M., Epstein, H., Romanovsky, V.E., Walker, D.A., 2008. High stocks of soil organic carbon in the North American Arctic region. *Nat. Geosci.* 1, 615–619.
- Cools, N., De Vos, B., 2010. Sampling and analysis of soil. Manual part X. In: *Manual on Methods and Criteria for Harmonized Sampling, Assessment, Monitoring and Analysis of the Effects of Air Pollution on Forests*. United Nations Economic Commission for Europe (UNECE), ICP Forests, Hamburg.
- Cunningham, S.C., Metzeling, K.J., Nally, R.M., Thomson, J.R., Cavagnaro, T.R., 2012. Changes in soil carbon of pastures after afforestation with mixed species: sampling, heterogeneity and surrogates. *Agric. Ecosyst. Environ.* 158, 58–65.

- Deng, L., Shangquan, Z., 2017. Afforestation drives soil carbon and nitrogen changes in China. *Land Degrad. Dev.* 28, 151–165.
- Duan, H.C., Wang, T., Xue, X., Liu, S.L., Guo, J., 2014. Dynamics of aeolian desertification and its driving forces in the Horqin Sandy Land, Northern China. *Environ. Monit. Assess.* 186, 6083–6096.
- FAO (FAO/IUSS Working Group WRB), 2006. World Reference Base for Soil Resources 2006; World Soil Resources Report. Rome, Italy, FAO, pp. 103.
- Feng, Q., Endo, K.N., Cheng, G., 2002. Soil carbon in desertified land in relation to site characteristics. *Geoderma* 106, 21–43.
- Foley, J.A., 1995. An equilibrium model of the terrestrial carbon budget. *Tellus Ser. B Chem. Phys. Meteorol.* 47, 310–319.
- Gao, P., Wang, B., Geng, G., Zhang, G., 2013. Spatial distribution of soil organic carbon and total nitrogen based on GIS and geostatistics in a small watershed in a hilly area of northern China. *PLoS One* 8, e83592.
- Gomez, C., Rossel, R.A.V., McBratney, A.B., 2008. Soil organic carbon prediction by hyperspectral remote sensing and field vis–NIR spectroscopy: an Australian case study. *Geoderma* 146, 403–411.
- Grüneberg, E., Ziche, D., Wellbrock, N., 2014. Organic carbon stocks and sequestration rates of forest soils in Germany. *Glob. Chang. Biol.* 20, 2644–2662.
- Guo, L.B., Gifford, R.M., 2002. Soil carbon stocks and land use change: a meta analysis. *Glob. Chang. Biol.* 8, 345–360.
- Jobbágy, E.G., Jackson, R.B., 2000. The vertical distribution of soil organic carbon and its relation to climate and vegetation. *Ecol. Appl.* 10, 423–436.
- Kern, J.S., 1994. Spatial patterns of soil organic carbon in the contiguous United States. *Soil Sci. Soc. Am. J.* 58, 439–455.
- Lal, R., 2001. Potential of desertification control to sequester carbon and mitigate the greenhouse effect. *Clim. Chang.* 51, 35–72.
- Lal, R., 2004a. Soil carbon sequestration impacts on global climate change and food security. *Science* 304, 1623–1627.
- Lal, R., 2004b. Soil carbon sequestration to mitigate climate change. *Geoderma* 123, 1–22.
- Li, Y.Q., Zhao, H.L., Zhao, X.Y., Zhang, T.H., Chen, Y.P., 2006. Biomass energy, carbon and nitrogen stores in different habitats along a desertification gradient in the semiarid Horqin Sandy Land. *Arid Land Res. Manag.* 20, 43–60.
- Li, Y.Q., Zhou, X.H., Brandle, J., Zhang, T.H., Chen, Y.P., Han, J.J., 2012. Temporal progress in improving carbon and nitrogen storage by grazing enclosure practice in a degraded land area of China's Horqin Sandy Grassland. *Agric. Ecosyst. Environ.* 159, 55–61.
- Li, Y.Q., Brandle, J., Awada, T., Chen, Y.P., Han, J.J., Zhang, F., Luo, Y.Q., 2013. Accumulation of carbon and nitrogen in the plant–soil system after afforestation of active sand dunes in China's Horqin Sandy Land. *Agric. Ecosyst. Environ.* 177, 75–84.
- Li, Y.Q., Han, J.J., Wang, S.K., Brandle, J., Lian, J., Luo, Y.Q., Zhang, F.X., 2014. Soil organic carbon and total nitrogen storage under different land uses in the Naiman Banner, a semiarid degraded region of northern China. *Can. J. Soil Sci.* 94, 9–20.
- Li, Y.Q., Chen, Y.P., Wang, X.Y., Niu, Y.Y., Lian, J., 2017. Improvements in soil carbon and nitrogen capacities after shrub planting to stabilize sand dunes in China's Horqin Sandy Land. *Sustainability* 9, 662.
- Liu, X.M., Zhao, H.L., Zhao, A.F., 1996. Characteristics of Sandy Environment and Vegetation in the Horqin Sandy Land. Science Press, Beijing, China (in Chinese).
- Liu, D., Wang, Z., Zhang, B., Song, K., Li, X., Li, J., Li, F., Duan, H., 2006. Spatial distribution of soil organic carbon and analysis of related factors in croplands of the black soil region, Northeast China. *Agric. Ecosyst. Environ.* 113, 73–81.
- Liu, Z., Shao, M., Wang, Y., 2011. Effect of environmental factors on regional soil organic carbon stocks across the Loess Plateau region, China. *Agric. Ecosyst. Environ.* 142, 184–194.
- Lorenz, K., Lal, R., 2005. The depth distribution of soil organic carbon in relation to land use and management and the potential of carbon sequestration in subsoil horizons. *Adv. Agron.* 88, 35–66.
- Luo, Z., Feng, W., Luo, Y., Baldock, J., Wang, E., 2017. Soil organic carbon dynamics jointly controlled by climate, carbon inputs, soil properties and soil carbon fractions. *Glob. Chang. Biol.* 23, 4430–4439.
- Ma, K., Zhang, Y., Tang, S., Liu, J., 2016. Spatial distribution of soil organic carbon in the Zoige alpine wetland, northeastern Qinghai–Tibet Plateau. *Catena* 144, 102–108.
- Martín, M.P., Wattenbach, M., Smith, P., Meersmans, J., Jolivet, C., Boulonne, L., Arruays, D., 2011. Spatial distribution of soil organic carbon stocks in France. *Biogeosciences* 8, 1053–1065.
- McGrath, D., Zhang, C., 2003. Spatial distribution of soil organic carbon concentrations in grassland of Ireland. *Appl. Geochem.* 18, 1629–1639.
- Mitra, S., Wassmann, R., Vlek, P.L.G., 2005. An appraisal of global wetland area and its organic carbon stock. *Curr. Sci.* 88, 25–35.
- Montes, C.R., Lucas, Y., Pereira, O.J.R., Achard, R., Grimaldi, M., Melfi, A.J., 2011. Deep plant-derived carbon storage in Amazonian podzols. *Biogeosciences* 8, 113–120.
- Nelson, D.W., Sommers, L.E., 1982. Total carbon, organic carbon and organic matter. In: Page, A.L., Miller, R.H., Keeney, D.R. (Eds.), *Methods of Soil Analysis*, Part 2, 2nd ed. American Society of Agronomy, Madison, WI, USA, pp. 539–577.
- Nosetto, M.D., Jobbágy, E.G., Paruelo, J.M., 2006. Carbon sequestration in semi-arid rangelands: comparison of *Pinus ponderosa* plantations and grazing exclusion in NW Patagonia. *J. Arid Environ.* 67, 142–156.
- O'Rourke, S.M., Angers, D.A., Holden, N.M., McBratney, A.B., 2015. Soil organic carbon across scales. *Glob. Chang. Biol.* 21, 3561–3574.
- Post, W.M., Kwon, K.C., 2000. Soil carbon sequestration and land-use change: processes and potential. *Glob. Chang. Biol.* 6, 317–328.
- Post, W.M., Emanuel, W.R., Zinke, P.J., Stangenberger, A.G., 1982. Soil carbon pools and world life zones. *Nature* 298, 156–159.
- RESDC, 2017. Resources and Environmental Sciences Data Center. Chinese Academy of Sciences Available online: <http://www.resdc.cn/>.
- Scharlemann, J.P., Tanner, E.V., Hiederer, R., Kapos, V., 2014. Global soil carbon, understanding and managing the largest terrestrial carbon pool. *Carbon Manage.* 5, 81–91.
- Schrumpf, M., Schulze, E.D., Kaiser, K., Schumacher, J., 2011. How accurately can soil organic carbon stocks and stock changes be quantified by soil inventories? *Biogeosciences* 8, 1193–1212.
- Smith, P., Fang, C.M., Dawson, J.J.C., Moncrieff, J.B., 2008. Impact of global warming on soil organic carbon. *Adv. Agron.* 97, 1–43.
- Tarnocai, C., Canadell, J.G., Schuur, E.A.G., Kuhry, P., Mazhitova, G., Zimov, S., 2009. Soil organic carbon pools in the northern circumpolar permafrost region. *Glob. Biogeochem. Cycles* 23, 2607–2617.
- Vågen, T.G., Winowiecki, L.A., Tondoh, J.E., Desta, L.T., Gumbricht, T., 2016. Mapping of soil properties and land degradation risk in Africa using MODIS reflectance. *Geoderma* 263, 216–225.
- Wang, S., Mei, H., Shao, X., Mickler, R.A., Li, K., Ji, J.J., 2004. Vertical distribution of soil organic carbon in China. *Environ. Manag.* 33, S200–S209.
- Wiesmeier, M., Spörlein, P., Geuß, U., Hangen, E., Haug, S., Reischl, A., Schilling, B., von Lützow, M., Kögel-Knabner, I., 2012. Soil organic carbon stocks in southeast Germany (Bavaria) as affected by land use, soil type and sampling depth. *Glob. Chang. Biol.* 18, 2233–2245.
- Wiesmeier, M., Munro, S., Barthold, F., Steffens, M., Schad, P., Kögelknabner, I., 2015. Carbon storage capacity of semi-arid grassland soils and sequestration potentials in northern China. *Glob. Chang. Biol.* 21, 3836–3845.
- Xie, Z.B., Zhu, J.G., Liu, G., Cadisch, G., Hasegawa, T., Chen, C.M., Sun, H.F., Tang, H.Y., Zeng, Q., 2007. Soil organic carbon stocks in China and changes from 1980s to 2000s. *Glob. Chang. Biol.* 13, 1989–2007.
- Yang, Y.H., Fang, J.Y., Tang, Y., Ji, C.J., Zheng, C., He, J.S., Zhu, B., 2008. Storage, patterns and controls of soil organic carbon in the Tibetan grasslands. *Glob. Chang. Biol.* 14, 1592–1599.
- Yang, Y.H., Fang, J.Y., Smith, P., Tang, Y.H., Chen, A.P., Ji, C.J., Hu, H.F., Rao, S., Tan, K., He, J.S., 2009. Changes in topsoil carbon stock in the Tibetan grasslands between the 1980s and 2004. *Glob. Chang. Biol.* 15, 2723–2729.
- Yu, D.S., Shi, X.Z., Wang, H.J., Sun, W.X., Chen, J.M., Liu, Q.H., Zhao, Y.C., 2007. Regional patterns of soil organic carbon stocks in China. *J. Environ. Manag.* 85, 680–689.
- Zhang, S., Huang, Y., Shen, C., Ye, H., Du, Y., 2012. Spatial prediction of soil organic matter using terrain indices and categorical variables as auxiliary information. *Geoderma* 171–172, 35–43.
- Zhou, R.L., Li, Y.Q., Zhao, H.L., Drake, S., 2008. Desertification effects on C and N content of sandy soils under grassland in Horqin, northern China. *Geoderma* 145, 370–375.